Proceedings in
Image Fusion and Shape Variability Techniques

International Conference, held in Leeds, UK, 3-5 July 1996,

incorporating The 16th Leeds Annual Statistical Research (L.A.S.R.) Workshop

co-sponsored by the Centre of Medical Imaging Research (CoMIR)

Edited by

K.V. Mardia, C.A. Gill, I.L. Dryden

Department of Statistics,

University of Leeds, Leeds LS2 9JT.

Leeds University Press

Front cover: An investigation of asymmetry of the human face using ridge curves, (see John T. Kent, Delman Lee, Kanti V. Mardia, Alf D. Linney pp88-99 of this volume).

ISBN 0 85316 173 9

Conference Committee

I.L. Dryden
C.A. Gill
J.T. Kent
K.V. Mardia

Department of Statistics

University of Leeds

Leeds, LS2 9JT, UK

Conference Organisers

I.L. Dryden
C.A. Gill
K.V. Mardia

Session Chairs

Session I
J.T. Kent
Department of Statistics, University of Leeds, Leeds LS2 9JT, UK.

Session II
K.V. Mardia
Department of Statistics, University of Leeds, Leeds LS2 9JT, UK.

Session III
Fred L. Bookstein
Centre for Human Growth & Development, University of Michigan,
Ann Arbor, Michigan 48109, USA.

Session IV
D.C. Hogg
School of Computer Studies, University of Leeds, Leeds LS2 9JT, UK.

PREFACE

The Leeds Annual Statistics Research (LASR) workshop has become firmly established as an international event. This year the 16th workshop focuses again on the interface between Statistics and Image Analysis. The interaction between the two subjects has led to many major advancements in the last fifteen years or so and our mission at Leeds continues to play an important part in the development of the fields. Summaries of the important advancements can be found in the special volumes Statistics and Images 1 and 2 (Carfax, Oxford 1993, 1994) edited by Mardia and Kanji, and Mardia respectively and in the Proceedings from last year's workshop 'Current Issues in Statistical Shape Analysis' (CISSA) (University of Leeds, 1995), edited by Mardia and Gill.

Why hold this year's workshop on "Image fusion and shape variability techniques"? Through our continued active role in CoMIR (Centre of Medical Imaging Research) many applications in fusing images from two modalities have arisen. The desire to match two or more different images is finding a diverse range of applications in many other fields and we thought it timely to hold our workshop on this theme. The study of shape and shape variability continues to be an important topic in image fusion and other areas of image analysis, both for prior modelling and for object recognition. Comparison and analysis of objects at a variety of scales can lead to powerful new approaches and some multi-scale and wavelet approaches will be described in this workshop. Also described will be the topic of warping, which is an important feature of fusion, averaging of images and measuring shape variability. We are delighted that several key researchers in these fields have agreed to participate in this workshop.

This collection of papers gives a flavour of the current topics of interest in the field. The Proceedings are, like last year, available at the workshop itself. Last year the volume was found to be a very useful source both at the workshop and afterwards. Authors are to be thanked for sending in their manuscripts (some of them on time!) and making this volume a comprehensive source that will be referred to in the future.

We are very grateful for the support of EPSRC enabling us to invite four of the keynote speakers: Professor Jan J. Koenderink, Professor Valen E. Johnson, Professor Demetri Terzopoulos and Dr. André Guéziec. We also acknowledge the support of CoMIR and the University of Leeds.

Kanti Mardia
Christine Gill
Ian Dryden
12-06-96

CONTENTS

PART II: POSTERS 203

A General Scheme for Automatically Building 3D Morphometric Anatomical Atlases: application to a Skull and a Brain Atlas

Gérard Subsol, Jean-Philippe Thirion and Nicholas Ayache
INRIA, 2 004 route des Lucioles, BP 93, 06 902 Sophia Antipolis Cedex, France
E-mail: Gerard.Subsol@epidaure.inria.fr

1 Introduction

If over the past few years, many digital anatomical atlases based on 3D medical images have been developed, very few of them include morphometric tools to estimate the variability in the shape of anatomical structures. We can cite the work described in [CHTH93] (description of brain structures and their variability), [CBH+93] and [CDB+95] (creation of a 3D morphometric skull atlas) or [BBW+94] (generation of a liver atlas for model-based segmentation). Nevertheless, these atlases are built from an a priori model: a "template" which was manually defined by anatomists.

In this paper, we address the new problem of automatically building morphometric anatomical atlases from volumetric medical images without any a priori knowledge. We think that with such an automatic process, we could handle with the very fine precision of medical images (voxel size of about 1 millimeter) and take into account many landmarks (several hundreds of points) from many data (several tens) in order to obtain very accurate morphometric parameters.

Let us assume we have a database of medical images of a given anatomical structure acquired from different patients. The problem is threefold: first, we have to extract landmarks in the different items of the database. Then, we have to find the correspondences between them in order, at the end, to compute some statistical parameters about their positions and their variabilities.

In the first part of this paper, we propose an algorithm to build a 3D morphometric anatomical atlas. Then, in the second part, we show some results about an atlas of the skull and the brain and how could they be used to assist medical diagnosis.

2 Description of the atlas construction scheme

2.1 Step 1: feature extraction

This step consists of automatically extracting in the 3D images the features which will constitute the atlas.

As features, we choose "crest lines" [MBF92] which are mathematically defined as the salient lines on a surface. Crest lines are as a simple representation of the studied anatomical structure (see Figure 1) and seem to be anatomically stable [GA92]. In particular, on the skull, they are

very close from "ridge lines" [BC88] defined by anatomists as it is emphasized in [TSD96]. On the brain, they seem to follow patterns of convolutions [OKA90]. Crest lines are automatically extracted by the "Marching Lines" algorithm [TG93] directly in the 3D image.

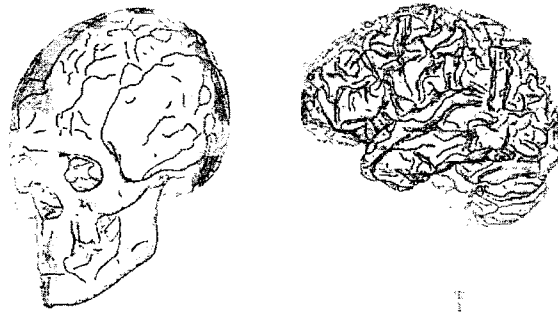

Figure 1: *Crest lines of a skull and of a brain.*

2.2 Step 2: common feature extraction

For each item of the database, we have a set of crest lines. We find correspondences between them (i.e. which line of one set corresponds to which line of the other) by using a non-rigid registration algorithm described in [STA95]. When we have the correspondences between the lines of all the items, we can identify which crest lines are generic, i.e. present in all the data sets. These common crest lines will form the structure of the atlas.

Moreover, if the lines of one item have been manually labelled, the labels can be automatically propagated to the lines of the other sets belonging to the same common subset.

As the registration is based only on geometrically defined features, we cannot be sure of the biological homology [DGB95]. Nevertheless, in [TSD96], we show that results of registration based on crest lines and "ridge lines" are similar.

2.3 Step 3: feature average

In order to obtain the positions of the features, we "average" the crest lines of the different items belonging to the same common subset.

But before, as emphasized in [DL89], we have to remove the rigid and isotropic scaling transformation between the items in order that the remaining differences between lines represent meaningful morphological differences. So, we choose an item of the database as the reference $\mathcal{R}$. Thanks to the registration results of the step 2, we can compute the global rigid and homothetic transformations between $\mathcal{A}$ and the other items and we apply them in order to have all the items in the same frame.

We have developed an algorithm that computes a "smooth" average of a set of tridimensional lines composed of tens or hundreds of points. For each line $\mathcal{L}$ of $\mathcal{R}$, we find the deformations

between $\mathcal{L}$ and the lines of the other items belonging to the same common subset. Then, we decompose them into a basis of fundamental deformations called modes by "modal analysis" technique [PS91] [NA94] [MPK94]. The amplitudes of the modes are averaged, defining a "mean" deformation which applied to $\mathcal{L}$ gives the "mean" line. The set of these mean lines constitutes the atlas.

What is particularly interesting in modal analysis is that in the same way as in Fourier analysis, we can approximate a deformation by taking into account just its few first modes. The truncation of the modal development is a kind of filtering, discarding high frequency deformations. We use this property in order to smooth 3D lines and reduce noise artefacts.

2.4 Step 4: feature deformation analysis

A statistical process is performed in order to quantify the variations of the features around their average position. In particular, it allows us to verify the "stability" of the locations of the features.

To analyse the deformations, we use modal decomposition as in [NA94] (application to cardiac deformations) and [MPK94] (shape analysis of brain structures).

By the same process as in step 3 (just replacing $\mathcal{R}$ by the atlas), we register each line l of the atlas with those of each item of the database, find the deformations and decompose them into modes. For each mode i, we compute the average amplitude d_i^l and the standard deviation σ_i^l. We can also compute the modes of the deformation $d_{\mathcal{S}}^l[i]$ between the same line l of the atlas and those of any new item $\mathcal{S}$ and compare their amplitudes according to d_i^l and σ_i^l by the *amplitude distance* (computed for the x, y and z axis):

$$dist(\mathcal{S}, l, i) = \sqrt{\frac{\left(d_{\mathcal{S}}^l[i] - d_i^l\right)^2}{\sigma_i^{l2}}}$$

Large values of $dist(\mathcal{S}, l, i)$ enable us to find the modes i characterizing the "abnormal" deformations.

3 Application to the skull

3.1 Construction of the atlas

In Figure 2, left, we display the set of mean common lines of the atlas computed from a database of six CT-Scan images of different skulls[1] [STA95].

Among all the common lines automatically detected are major anatomical landmarks as the orbits, the nose, the cheekbones, the temples or the mandible. Inside the skull, we also find crest lines following the magnum foramen, the sphenoid and the temporal bones. Moreover, we can notice how the atlas is symmetric.

With a spline based technique [DSTA95], we warp the surface of the reference skull according to the registration between its lines and the atlas lines in order to obtain the surface representation of the average skull which is displayed in Figure 2, right. This atlas representation is visually very similar to the one presented in [CBH+93]

[1] CT-Scan data of the skulls (120 slices of 256 x 256 pixels) from the Cleveland Museum of Natural History and General-Electric Medical System Europe.

Figure 2: *Left: the skull atlas of crest lines computed from a database of 6 different skulls. Right: a surface representation.*

3.2 Study of a maxillary deformation

In this section, we use the atlas in order to study a skull[2] $\mathcal{S}$ affected by a significant maxillary hypoplasia (see Figure 3, left).

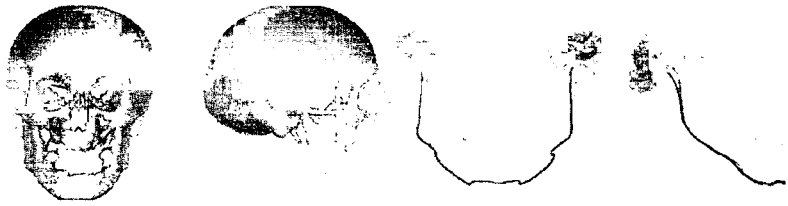

Figure 3: *Left: the skull $\mathcal{S}$ with a significant maxillary hypoplasia. Right: the mandible of $\mathcal{S}$ was automatically labelled and extracted thanks to the registration with the atlas (in black, the mandibular crest line).*

By registering the crest lines of the atlas with those of $\mathcal{S}$, we are able to automatically label these latter, identifying, in particular, the mandibular line. By taking points of the surface which are close to this line, we can automatically extract the mandible of $\mathcal{S}$ (see Figure 3, right).

With the pairs of matched points found by the registration between the atlas and $\mathcal{S}$, we can compute the rigid and homothetic transformations which best superimpose (in a least-squares sense) the two skulls (see Figure 4, left). By this way, we are able to contrast $\mathcal{S}$ and the atlas and emphasize the deformations of the mandible which appears laterally too wide and vertically stretched. The surgeon could use this superimposed display to estimate his surgical procedures.

Let us analyze now quantitatively the deformations of the mandible. With the method described in the step 4, we compute the amplitude distances of the 5 first modes of the $\mathcal{S}$ mandibular line deformation (see Table I) according to the atlas. If we threshold the values by 2 (corresponding to a variation of 2 standard deviations around the mean value), we notice that the 1^{st}, 2^{nd} x-mode and the 4^{th} z-mode amplitude distances are not in the statistics bounds. The

[2]CT-Scan data of the skull (135 slices of 256×256 pixels) have been obtained by Dr. David Dean (Case Western University of Cleveland) from the Naturhistorisches Museum of Vienna.

corresponding deformations can be considered as typical of the mandibular "abnormality"

	Mode 0	Mode 1	Mode 2	Mode3	Mode 4
x	0.124	2.442	2.476	0.745	0.353
y	0.906	0.759	1.601	1.734	0.920
z	1.806	0.896	1.062	1.017	2.267

Table 1: *Amplitude distances for the 5 first modes of the mandibular crest line deformation between S and the atlas. The 1^{st}, $2^{nd}x$-mode as the $4^{th}z$-mode are detected as "abnormal"*

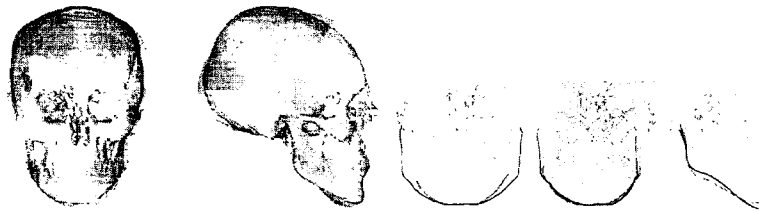

Figure 4: *Left: rigid and scale registration of the atlas (in solid) with S (in transparency) emphasizing the deformations of the mandible. Right: the three "abnormal" basic deformations of the S mandible: the 1^{st} x-mode which quantifies the breadth of the mandible, the 2^{nd} x-mode which represents the vertical twist of the mandible and the 4^{th} z-mode which characterizes the lateral curvature.*

In order to visualize these abnormal basic deformations, we deform the atlas mandible according to the three modes (with an amplitude multiplied by 3). From Figure 4, right, we can conclude that the $1^{st}x$-mode represents the *breadth* of the mandible. The effect of the $2^{nd}x$-mode is not symmetrical. In fact, the mandible appears slightly skew and this mode represents its *vertical twist*. The $4^{th}z$-mode represents the *lateral curvature* of the mandible.

3.3 Application to the brain

3.4 Construction of the atlas

The brain atlas was computed from a database of 10 MR head images[3] [STA96a]. Due to the huge shape complexity and interindividual variability of the cortical surface, we obtain less common crest lines than for the skull (see Figure 5). Nevertheless, we can notice how crest lines underline correctly the cerebral ventricles.

[3]MRI data (123 slices of 256 x 256 pixels) where the brains were manually segmented by courtesy of Dr. Ron Kikinis from the Brigham & Women's Hospital and Harvard Medical School of Boston.

Figure 5: *Left and center: the mean common lines constituting the brain atlas. Right: notice how the lines underline the cerebral ventricles.*

3.5 Study of cerebral ventricles shape

In this section, we use the atlas to study an individual brain[4] $\mathcal{CE}$, in particular, its cerebral ventricles. Their deformations can be characteristic of Alzheimer's disease or hydrocephalus [MPK94].

First, we perform an automatic segmentation by mathematical morphology and thresholding tools to obtain the cortical surface presented in Figure 6, left. Then, we register the crest lines of the brain atlas with those of $\mathcal{CE}$. We propagate the atlas labels to $\mathcal{CE}$ in order to identify some structures, in particular the cerebral ventricles (see Figure 6, right).

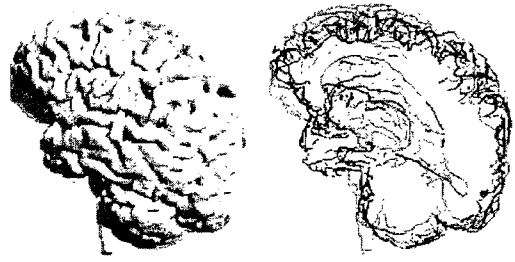

Figure 6: *Left: automatic segmentation of the cortical surface from a MRI of the head. Right: crest lines extracted on the cortical surface and the ventricles.*

With the pairs of matched points found by the registration between the atlas and $\mathcal{CE}$, we compute the rigid and homothetic transformations which best superimpose (in a least-squares sense) the two brains (see Figure 7, left). This superimposition shows that the patient ventricles are bigger and asymmetric (the left ventricle is larger).

We can analyze the deformations of the longest atlas ventricular line. We decompose its deformation towards the patient ventricular lines and compute the amplitude distances for the first

[4] MRI data of the head (254 slices of 256×256 pixels) have been obtained by Dr. Neil Roberts from the Magnetic Resonance Research Centre, University of Liverpool.

	Mode 0	Mode 1	Mode 2	Mode 3	Mode 4
Left x	-0.447	-5.125	+1.908	-2.140	-1.907
Right x	-1.026	+4.368	-2.254	+1.603	4.723
Left y	-3.687	+8.667	+0.451	+0.736	-5.081
Right y	-1.242	+8.336	-0.999	+0.757	-5.233
Left z	+4.429	-1.287	-3.731	-0.186	-1.442
Right z	+0.309	+1.824	-5.590	+1.986	-0.581

Table 2: *Amplitude distances for the 5 first modes of the deformation of the longest left and right ventricular crest line deformation between $C\mathcal{E}$ and the atlas. The framed modes are detected as "abnormal"*

5 modes. Significant deformations are those which are further than 3 standard deviations from the average value (see Table 2).

If we do not consider the mode 0 which corresponds to the translation, we notice how "abnormal" modes tend to apply simultaneously to left and right ventricles (with different amplitudes). It proves that both ventricles are "affected" by the deformations. The y and z "abnormal" modes have the same sign, so they are oriented in the same sense. On the contrary, x "abnormal" modes have opposite sign and the deformations are in inversed directions. If we only consider the first deformation mode which is the more global one, we notice that the x, y amplitudes are larger for the left ventricle. It tends to prove that the two ventricles are asymmetric and that the left one is the largest.

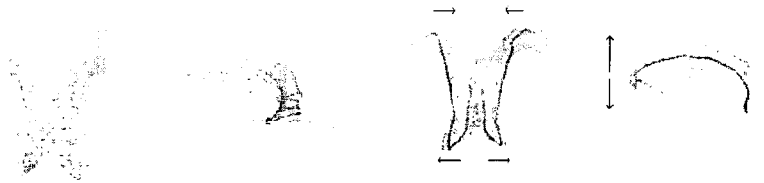

Figure 7: *Left: qualitative study of $C\mathcal{E}$ (in transparency) ventricles by superimposition with those of the atlas (in solid). Right: quantitative study of the ventricles deformation by analysis of the deformations and decomposition in "abnormal" modes ($1x$ and $1y$ modes).*

Now, let us study more specifically the two "abnormal" modes $1x$ and $1y$. For that purpose, we apply successively to the atlas line the 2 modes and we visualize the results in Figure 7, right: he parameter $1x$ models the *horizontal curvature* and the parameter $1y$ measures the *vertical enlargement*.

4 Conclusion

By automatically building 3D morphometric anatomical atlases, we have been able to obtain statistical parameters which could be useful to assist medical diagnosis. In particular, "abnormal" shape deformation can be automatically detected and quantified by a very reduced set of parameters.

Our future work will focus on studying other statistical tools for shape description (for example, Thin-Plate Splines [Boo91], Principal Component Analysis [CHTH93] or Fourier descriptors [SKBG95]), using other types of lines [SBK+92], developing other applications as the study of the growth of a child head [STA96b] or the hominin evolution [Dea93], working on larger databases and validating our first results on a anatomical and medical basis.

References

[BBW+94] J.L. Boes, P.H. Bland, T.E. Weymouth, L.E. Quint, F.L. Bookstein, and C.R. Meyer. Generating a Normalized Geometric Liver Model Using Warping. *Investigative Radiology*, 29(3):281–286, 1994.

[BC88] F. L. Bookstein and C. B. Cutting. A proposal for the apprehension of curving craniofacial form in three dimensions. In K. Vig and A. Burdi, editors, *Craniofacial Morphogenesis and Dysmorphogenesis*, pages 127–140, 1988.

[Boo91] F. L. Bookstein. Thin-Plate Splines and the Atlas Problem for Biomedical Images. In A. C. F. Colchester and D. J. Hawkes, editors, *Information Processing in Medical Imaging*, number 511 in Lecture Notes in Computer Science, pages 326–342, Wye (UK), July 1991. Springer-Verlag.

[CBH+93] C. B. Cutting, F. L. Bookstein, B. Haddad, D. Dean, and D. Kim. A spline-based approach for averaging three-dimensional curves and surfaces. In David C. Wilson and Joseph N. Wilson, editors, *Mathematical Methods in Medical Imaging II 1993*, pages 29–44, San Diego, California (USA), July 1993. SPIE.

[CDB+95] C. Cutting, D. Dean, F.L. Bookstein, B. Haddad, D. Khorramabadi, F. Z. Zonneveld, and J.G. Mc Carthy. A Three-dimensional Smooth Surface Analysis of Untreated Crouzon's Disease in the Adult. *Journal of Craniofacial Surgery*, 6:1–10, 1995.

[CHTH93] T.F. Cootes, A. Hill, C.J. Taylor, and J. Haslam. The Use of Active Shape Models For Locating Structures in Medical Images. In H. H. Barrett and A.F. Gmitro, editors, *Information Processing in Medical Imaging*, pages 33–47, Flagstaff, Arizona (USA), June 1993. IPMI'93, Springer-Verlag.

[Dea93] D. Dean. *The Middle Pleistocene Homo erectus/Homo sapiens Transition: New Evidence from Space Curve Statistics*. PhD thesis, The City University of New York, 1993.

[DGB95] D. Dean, A. Guéziec, and Cutting C. B. Homology and the Criteria for Building Deformable Templates. In K. V. Mardia and C. A. Gill, editors, *Current Issues in Statistical Shape Analysis*, pages 202–205, Leeds (United Kingdom), 1995. University of Leeds Press.

[DL89] B. David and B. Laurin. Déformations ontogénétiques et évolutives des organismes : l'approche par la méthode des points homologues. *C. R. Académie des Sciences Paris*, II(309):1271–1276, 1989.

[DSTA95] J. Declerck, G. Subsol, J.Ph. Thirion, and N. Ayache. Automatic retrieval of anatomical structures in 3D medical images. In N. Ayache, editor, *CVRMed'95*, volume 905 of *Lecture Notes in Computer Science*, pages 153–162, Nice (France), April 1995. Springer Verlag.

[GA92] A. Guéziec and N. Ayache. Smoothing and Matching of 3-D Space Curves. In *Visualization in Biomedical Computing*, pages 259–273, Chapel Hill, North Carolina (USA), October 1992. SPIE.

[MBF92] O. Monga, S. Benayoun, and O. D. Faugeras. Using Partial Derivatives of 3D Images to Extract Typical Surface Features. In *CVPR*, 1992.

[MPK94] J. Martin, A. Pentland, and R. Kikinis. Shape Analysis of Brain Structures Using Physical and Experimental Modes. In *Computer Vision and Pattern Recognition*, pages 752–755, Seattle, Washington (USA), June 1994.

[NA94] Ch. Nastar and N. Ayache. Classification of Nonrigid Motion in 3D Images using Physics-Based Vibration Analysis. In *IEEE Workshop on Biomedical Analysis*, pages 61–69, Seattle (USA), June 1994.

[OKA90] M. Ono, S. Kubik, and Ch. D. Abernathey. *Atlas of the Cerebral Sulci*. Georg Thieme Verlag, 1990.

[PS91] A. Pentland and S. Sclaroff. Closed-Form Solutions for Physically Based Shape Modeling and Recognition. *IEEE Transactions on Pattern Analysis and Machine Intelligence*, 13(7):715–729, July 1991.

[SBK+92] G. Székely, Ch. Brechbühler, O. Kubler, R. Ogniewicz, and T. Budinger. Mapping the human cerebral cortex using 3D medial manifolds. In Richard A. Robb, editor, *Visualization in Biomedical Computing*, pages 130–144, Chapel Hill, North Carolina (USA), October 1992. SPIE.

[SKBG95] G. Székely, A. Kelemen, Ch. Brechbuhler, and G. Gerig. Segmentation of 3D Objects from MRI Volume Data Using Constrained Elastic Deformations of Flexible Fourier Surface Models. In N. Ayache, editor, *CVRMed'95*, volume 905 of *Lecture Notes in Computer Science*, pages 495–505, Nice (France), April 1995. Springer-Verlag.

[STA95] G. Subsol, J. Ph. Thirion, and N. Ayache. A General Scheme for Automatically Building 3D Morphometric Anatomical Atlases: application to a Skull Atlas. In *Medical Robotics and Computer Assisted Surgery*, pages 226–233, Baltimore, Maryland (USA), November 1995.

[STA96a] G. Subsol, J. Ph. Thirion, and N. Ayache. Application of an Automatically Built 3D Morphometric Brain Atlas: Study of Cerebral Ventricle Shape. In K. H. Höhne, editor, *VBC'96*, Lecture Notes in Computer Science, Hamburg (Germany), September 1996. Springer Verlag.

[STA96b] G. Subsol, J. Ph. Thirion, and N. Ayache. Some applications of an automatically built 3D morphometric skull atlas. In H. Lemke, K. Inamura, A. Farman, and F. Vannier, editors, *Computer Assisted Radiology*, Paris (France), June 1996.

[TG93] J.Ph. Thirion and A. Gourdon. The Marching Lines Algorithm : new results and proofs. Technical Report 1881, INRIA, March 1993. Available by anonymous ftp at ftp.inria.fr /INRIA/tech-reports/RR.

[TSD96] J. Ph. Thirion, G. Subsol, and D. Dean. Cross Validation of Three Inter-Patients Matching Methods. In K. H. Höhne, editor, *VBC'96*, Lecture Notes in Computer Science, Hamburg (Germany), September 1996. Springer Verlag.